INSTITUTE OF PHYSICS PUBLISHING JOURNAL OF PHYSICS B: ATOMIC, MOLECULAR AND OPTICAL PHYSICS

J. Phys. B: At. Mol. Opt. Phys. **34** (2001) 3193–3203 PII: S0953-4075(01)24665-3

Complementary TDCS for the photo-double ionization of He at 40 eV above the threshold in unequal energy-sharing conditions

P Bolognesi[1], R Camilloni[1], M Coreno[2], G Turri[2,3,6], J Berakdar[4], A S Kheifets[5] and L Avaldi[1]

[1] CNR-IMAI, Area della Ricerca di Roma, CP10, 00016 Monterotondo Scalo, Italy
[2] INFM, Laboratorio TASC, Area Science Park, Basovizza, Trieste, Italy
[3] Dipartimento di Fisica, Politecnico di Milano, Milano, Italy
[4] Max-Planck Institüt fur Mikrostrukturphysik, Weinberg 2 D-06120 Halle(Saale), Germany
[5] Research School of Physical Sciences and Engineering, Australian National University, Canberra, ACT 2000, Australia

Received 8 May 2001, in final form 26 June 2001
Published 23 July 2001
Online at stacks.iop.org/JPhysB/34/3193

Abstract

Photo-double ionization (PDI) of helium at 40 eV above the threshold has been studied for unequal energy-sharing in the complementary kinematics obtained in two measurements by the interchange of the kinetic energies $E_1 \leftrightarrow E_2$ of the two photoelectrons. The triple differential cross sections (TDCS) were measured in the plane perpendicular to the photon direction using the multicoincidence end-station of the gas-phase photoemission beam-line of the Elettra storage ring. The measured TDCSs were compared with previous experimental results using a practical parametrization proposed by Cvejanovic and Reddish (2000 *J. Phys. B: At. Mol. Opt. Phys.* **33** 4691) and with predictions of the 3C and convergent close-coupling calculations. Satisfactory agreement with the previous experimental data was found. The comparison with the two theoretical models shows that the TDCSs is the complementary kinematics still present a challenge for PDI theory.

1. Introduction

In photo-double ionization (PDI) a single-incident photon produces two photoelectrons that escape from the residual doubly charged ion core. Due to the single-particle nature of the dipole interaction, the electric field of the photon can act on a single electron only. The transfer of the photon energy to the second electron is then controlled by electronic correlation. A vanishing interaction between the two photoelectrons leads to single photoemission only and

[6] Present address: Western Michigan University and Lawrence Berkeley National Laboratory, ALS Division, 1 Cyclotron Road MS 7-222 Berkeley, CA 94720, USA.

hence to a vanishing PDI signal. Thus the PDI is an ideal tool to trace the characteristics of the correlated motion of electronic systems. In this paper we focus on the PDI of helium, which represents the archetype of the three-body Coulomb problem (two interacting electrons coupled to a positive residual ion with no internal structure). The PDI investigation provides many challenges to both experimentalists and theorists alike. Since the reaction depends upon electron correlations, its total cross section is very small ($\widetilde{=}10^{-21}$ cm^2 at 1 eV above threshold [1]). Moreover, a complete characterization of the process implies the detection of the two photoelectrons in coincidence after energy and angular selection. In such an experiment the triple differential cross section (TDCS) $\mathrm{d}^3\sigma/\mathrm{d}\Omega_1\,\mathrm{d}\Omega_2\,\mathrm{d}E_1$, i.e. a cross section differential in the angles of emission of the two photoelectrons $\Omega_1 = (\vartheta_1, \varphi_1)$ and $\Omega_2 = (\vartheta_2, \varphi_2)$ and in one kinetic energy, is measured. The kinetic energy E_2 of the other electron is determined by energy conservation $h\nu - IP^{2+} = E = E_1 + E_2$, where IP^{2+} is the double ionization potential and E is the excess energy. In the energy balance the translational energy of the target atom and the recoil energy of the ion after the emission of the two electrons has not been accounted for, since they can be neglected due to the thermal target atoms. An alternative experimental approach to measure the TDCS is provided by the COLTRIMS method [2], in which the He^{2+} recoil ion and one of the two photoelectrons are detected in coincidence. In this method the measurements of the five or six components (depending on the time structure of the photon beam) of the two momenta allows one to determine the full kinematics of the PDI process. The low value of the cross section, the need for an energetic and tuneable photon source and the intrinsic difficulties of coincidence experiments have hampered the measurement of the TDCS of the PDI process for a long time. On the theoretical side, the correlated motion of the two electrons emerging from the atom needs to be described and a proper correlated initial-state wavefunction has to be used in order: (i) to calculate the patterns of the coincidence angular distribution as a function of E and of the energy sharing between the two electrons; and (ii) to predict the absolute values of the measured TDCS. Considerable progress has been made in the theoretical description of the three-body Coulomb problem, however, a universally applicable theory has not yet been proposed.

The first experimental investigation of the PDI in He has been performed by Schwarzkopft *et al* [3] in 1993 at 20 eV above the threshold in an equal energy-sharing condition ($E_1 = E_2$). Since then several measurements have been reported in the literature. They extend from the threshold [4, 5] up to 80 eV above the threshold [6]. The main experimental achievements in the study of two-electron processes in the threshold region and the experimental and theoretical results for the PDI of He atoms have been recently reviewed [7, 8], and will not be repeated here.

By considering the invariance with respect to the rotation around a preferential symmetry axis (for example, the electric vector direction of the incident radiation) and the general properties of the spherical harmonics the TDCS can be written in a way that allows full separation of the geometrical factors and the dynamical parameters, as shown in a very general way by Briggs and Schmidt [7]. This leads to a parametrization of the TDCS, first proposed by Huetz *et al* [9], which is particularly useful for experimentalists, because it can be easily linked to the experimental observations. In the case of an incident radiation that propagates along the z axis and is linearly polarized along the $\varepsilon = \varepsilon x$ axis the TDCS can be written as

$$\mathrm{TDCS}(E_1, E_2, \vartheta_{12}) \propto |a_\mathrm{g}(E_1, E_2, \vartheta_{12})(\cos\vartheta_1 + \cos\vartheta_2) + a_\mathrm{u}(E_1, E_2, \vartheta_{12}) \times (\cos\vartheta_1 - \cos\vartheta_2)|^2 \tag{1}$$

where ϑ_1 and ϑ_2 are the angles of emission of the two photoelectrons with respect to ε and ϑ_{12} is the relative angle between the directions of emission of the two photoelectrons. The complex amplitudes a_g and a_u are respectively symmetric and antisymmetric relative to the

exchange of E_1 and E_2. The ϑ_{12} and E dependence of these amplitudes includes all the physical information on the dynamics of the process, i.e. the effects of the electron–electron and electron–residual ion interactions. Most of the experimental attention has been paid to the study of the TDCS in the case of equal energy sharing. In such a case $a_u = 0$, thus the TDCS reduces to a simple form and does not display any circular dichroism [7]. The symmetry constraints of the process, expressed by the selection rules [7], then reduce the TDCS to a simple shape with characteristic nodes. Several studies of the PDI in equal energy-sharing conditions have been reported ([4–7] and references therein). The main challenge today is to produce absolute values for the TDCS, which can discriminate among the different models thus predicting similar TDCS patterns but different magnitudes.

The situation regarding the case of experiments in unequal energy sharing is quite different. With these kinematics both the a_g and a_u amplitudes contribute to the TDCS and the effects of circular dichroism are expected to occur for non-vanishing circular polarization of the light [7]. Thus a precise knowledge of the light polarization is vital, unless undulator radiation, which is fully linearly polarized in odd harmonics, is used. In the case of unequal energy sharing it is instructive to study the complementary TDCS patterns obtained in two experiments by the interchange of the electron kinetic energies, $E_1 \leftrightarrow E_2$. Due to the symmetrical properties of a_g and a_u the parametric expression of the TDCS in the two complementary cases will differ by the sign in front of the second addendum of (1). Complementary TDCS have been investigated only from the near threshold region [10, 11] up to about 20 eV [11, 12] above threshold. Moreover, the predictions of the different theories differ widely when the coincidence angular distribution of the slow electrons with the fast ones detected at a fixed direction is considered [7]. Here we present a study of the complementary TDCS for $E = 40$ eV and a reasonably large ratio between the kinetic energies of the two electrons: $E_1 \leftrightarrow E_2 = 5 \leftrightarrow 35$ eV, that correspond to $R = E_2/E_1 = 7$ and $1/7$. In the following the electron measured at a fixed direction will always be labelled as '1'. An excess energy of 40 eV has been chosen since according to previous works [7, 13] with this amount of excess energy it may be expected that the single electron behaviour dominates over the two-electron correlated emission. In other words, in this region it is reasonable to assume that one electron absorbs the photon and the other one shakes off [7] in the continuum. This can be seen by the U-shape of the energy distribution of the electrons [13] and in the different TDCSs depending on whether $E_1 < E_2$ or $E_1 > E_2$. Moreover, earlier TDCS measurements at $E_1 = 5$ eV and $E_2 = 35$ eV were reported by the Newcastle group [14]. On the one hand, the results of these two different experiments can be compared to rule out any systematic errors in the measured TDCS. On the other hand they can be combined to form a consistent and broad set of data to be used for a more stringent comparison with theoretical predictions.

2. Experimental

The experiment has been performed at the gas phase photoemission beam-line of the Elettra storage ring. The light source is an undulator of period 12.5 cm, 4.5 m long. The radiation from the undulator is deflected to the variable-angle spherical grating monochromator [15] by a prefocusing mirror. The monochromator consists of two optical elements: a plane mirror and a spherical grating. Four interchangeable gratings cover the energy region 20–1000 eV. Two refocusing mirrors after the exit slits provide a circular focus at the interaction region in the multicoincidence end-station [16] used in these experiments. The end-station is lined with a 2 mm-thick μ-metal shield. This shield together with coils near the main flanges result in a residual magnetic field of less than 10 mG in the experimental chamber. Two independently rotatable turntables are housed in the chamber. Seven spectrometers are mounted at 30° angular

intervals on a turntable that rotates in the plane perpendicular to the direction, z, of propagation of the incident radiation, while three other spectrometers are mounted at 0°, 30° and 60° with respect to the polarization vector ε of the light on a smaller turntable. This turntable can be rotated from the perpendicular plane to the (z, x) plane. In these measurements both the arrays have been kept in the perpendicular plane.

Each electrostatic spectrometer is composed of four element cylindrical lenses that focus the photoelectrons from the target region onto the entrance slit of the hemispherical deflector. The mean radius of the hemispherical deflector is 33 mm and the gap is 9.9 mm. In these measurements two rectangular slits of 2×4 mm^2 (2 mm is the size of the slit in the dispersion plane) have been used at the entrance and exit of the hemispherical deflector. The energy resolution and the angular acceptance in the dispersion plane of the spectrometers were $\Delta E/E_{1,2} = 0.03$ and $\pm 3°$, respectively. This small angular acceptance and the absence of sharp features in the TDCS enables us to compare the experimental results with the theoretical predictions without any convolution of the latter. Ceramic channeltrons (Dr Sjuts Optotechnik GmbH) are placed at the exit of the hemispherical deflectors to count the angular and energy-selected photoelectrons. The channeltron pulses after being amplified and discriminated are sent to the coincidence electronics, made by three independent time-to-digital converters, TDC. In the experiment each TDC unit is operated in the common-start mode with the signal of one of the three analysers of the small turntable used as the start and the signals from the other seven as the stop. In this way 21 coincidence pairs are collected simultaneously. The angular distribution is obtained by successive rotations of the larger frame. A PC equipped with Labview software (National Instruments) sets the voltages of the spectrometers, collects the non-coincidence and coincidence data and monitors the flux of the incident beam. The relative efficiency of the spectrometers has been calibrated via the measurement of the photoelectron angular distribution of $He^+(n = 3)$ and of $Kr^+(3\,d^{-1})$ at 5 and 35 eV above their thresholds, respectively. At these energies the β values are known [17, 18]. The efficiencies obtained were confirmed by determining the β of the photoelectron angular distribution of $He^+(1s^{-1})$ at the same kinetic energies. The same efficiency correction has been assumed for the coincidence measurements. The validity of this assumption was tested by measuring the coincidence yield at two positions of the larger turntable, which overlaps the two analysers nearby. Therefore all the experimental data are internormalized and can be reported on the same relative scale. This can be checked by observing that the same coincidence yield is measured for different configurations of the spectrometers, obtained by the interchange of energies and angles (for example, $[E_1 = 5$ eV , $E_2 = 35$ eV, $\vartheta_1 = 30°$ and $\vartheta_2 = 180°]$ and $[E_1 = 35$ eV , $E_2 = 5$ eV, $\vartheta_1 = 0°$ and $\vartheta_2 = 150°]$), which correspond to the same kinematics.

The experiment was performed at $h\nu = 119$ eV, using the first harmonic of the undulator. The odd harmonics of the radiation emitted by the undulator are expected to be completely linearly polarized. This has been checked by measuring the photoelectron angular distribution of He^+ $(n = 2)$ at the same photon value. A value of the Stokes parameter S_1 of 1.00 ± 0.03 was found.

At a photon intensity of 1.4×10^{13} photons s^{-1} (measured by a IRS photodiode placed behind the end-station) and an operating pressure in the chamber of 8×10^{-5} Torr, corresponding to an estimated target density of 10^{13} atom cm^{-3} in the interaction region, typical coincidence rates of 10 mHz per pair of detectors were obtained. The total acquisition time was 10 h per each complementary kinematics.

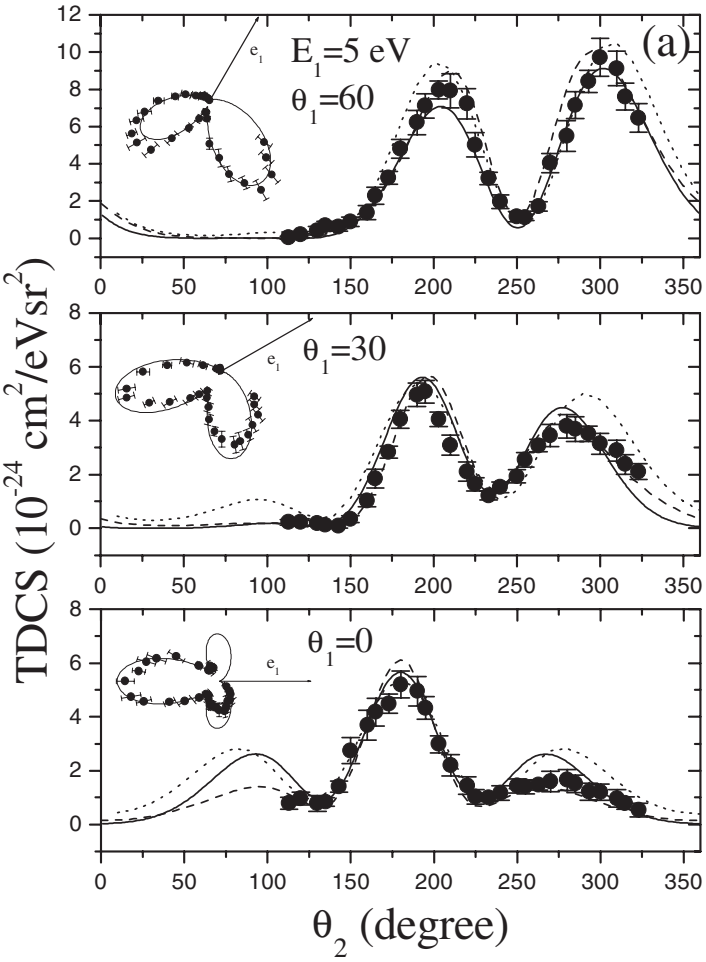

Figure 1. The He TDCS for $E = 40$ eV, $E_1 = 5$ eV and $E_2 = 35$ eV (*a*) and $E_1 = 35$ eV and $E_2 = 5$ eV (*b*). The experimental TDCSs are compared with the velocity-form predictions of the CCC model (dashed curve) and the 3C model (dotted curve). The full curve is the fit to the TDCS with the *practical parametrization* of [20] with four parameters. The values of the parameters are reported in table 1 and discussed in the text. In the top-left corner of each panel the experimental data are also represented by polar plots and compared with the results of the fit using the *practical parametrization* [20] with four parameters. For $E_1 = 5$ eV and $\vartheta_1 = 30^\circ$ the results of the parametrization were rescaled by 0.88, while both the 3C and CCC calculations were rescaled by 0.62 for $E_1 = 5$ eV and $\vartheta_1 = 30^\circ$ and 0°.

3. Results and discussion

The results of the measurements are reported in figures 1(*a*) and (*b*) with the differences

$$\Delta = \mathrm{TDCS}\,(E_1 = 35\ \mathrm{eV}, E_2 = 5\ \mathrm{eV}) - \mathrm{TDCS}\,(E_1 = 5\ \mathrm{eV}, E_2 = 35\ \mathrm{eV})$$
$$= 4|a_\mathrm{g}||a_\mathrm{u}|\cos\delta(\cos^2\vartheta_1 - \cos^2\vartheta_2) \qquad (2)$$

where δ is the relative phase of the amplitudes, being shown in figure 2.

The measurements at $E_1 = 5$ eV and $\vartheta_1 = 0$ and 30° (figure 1(*a*)) have also been performed by the Newcastle group, see figure 7 in [14] (the angles of [14] are related to the

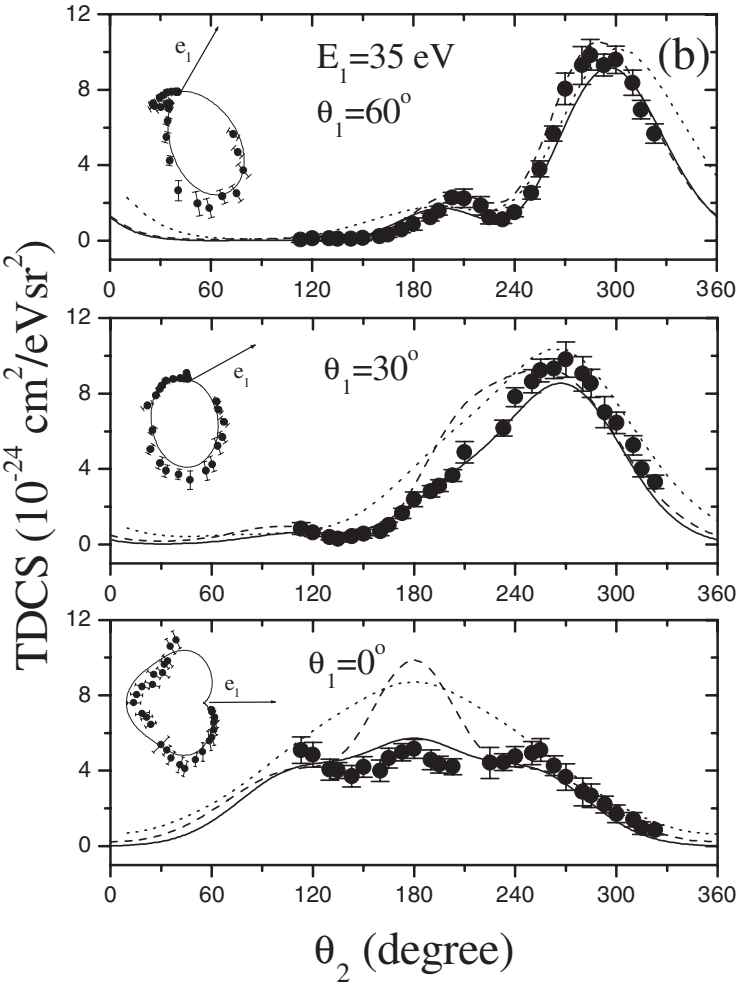

Figure 1. (Continued.)

present ones by the relation $180^\circ - \vartheta_1$). When comparing the two sets of experimental TDCS, the angular acceptances, the averaging over different angle segments and the polarization of the incident radiation have to be accounted for and thus such a comparison is not straightforward. The shapes of the TDCS measured in the two experiments are in good agreement. The better definition of the minima between the lobes observed in the present measurements and the slight shift of the secondary maxima at $\vartheta_1 = 0^\circ$ can in part be explained for by the different polarization of the light in the two experiments ($S_1 = 0.8$ and 1 in [14] and in this paper, respectively). The averaging over 10° segments in both ϑ_1 and ϑ_2 operated on the data collected with the toroidal analyser [14] does not introduce any further effects [19]. A more effective comparison between the two sets of data can be done using a *practical parametrization* of the TDCS proposed by Cvejanovic and Reddish [20]. This parametrization, based on the features of the gerade amplitude, relies on the assumption that the angular-correlation function is insensitive to the symmetry (gerade $\leftrightarrow$ ungerade) and to the electron-energy sharing. These two factors only affect the ratio between the two amplitudes, $\eta(E, R)$, and their relative phase

Table 1. The values of the Γ, η and δ parameters as obtained by a fit of the present data (see text) and in [20] to the kinematics with $E_1 = 5$ eV ($R = 7$). In the last column the values obtained by fitting the parametric expression of the amplitudes to the CCC calculation are reported.

	[14, 20]	This work,	This work, four parameters		CCC	
	Gerade	three parameters	Gerade	Ungerade	Gerade	Ungerade
$\vartheta_{1/2}(E = 40\text{ eV})$	98 ± 1	102 ± 1	104 ± 1	76 ± 2	98	72
$\eta(E = 40\text{ eV}, R = 7)$	0.25 ± 0.01	0.25 ± 0.01	0.25 ± 0.01		0.28	
$\delta(E = 40\text{ eV}, R = 7)$	$\pm 246^\circ \pm 4^\circ$[a]	$\pm 232^\circ \pm 2^\circ$[a]	$\pm 229^\circ \pm 2^\circ$[a]		243	

[a] $\delta(E = 40\text{ eV}, R = 7) = \delta(E = 40\text{ eV}, R = 1/7) + \pi$ [20].

$\delta(E, R)$. Both the amplitudes are represented by Gaussian functions and only three parameters, the correlation width $\vartheta_{1/2}(E)$, $\eta(E, R)$ and $\delta(E, R)$, in the simplest formulation

$$a_g(E, R, \vartheta_{12}) = a_g(E, R = 1, \vartheta_{12}) = \exp\left(\frac{-2\ln 2\,(\vartheta_{12} - 180^\circ)^2}{\vartheta_{1/2}^2}\right)$$
$$a_u(E, R, \vartheta_{12}) = \eta\,(E, R)\,e^{i\delta(E,R)} \exp\left(\frac{-2\ln 2\,(\vartheta_{12} - 180^\circ)^2}{\vartheta_{1/2}^2}\right) \tag{3}$$

or four parameters, allowing for different $\vartheta_{1/2}(E)$ values in the gerade and ungerade terms, are needed in the TDCS representation. Thus the *practical parametrization* facilitates comparisons between different sets of data, taken in a variety of kinematics, using only three or four parameters.

The values of the parameters in equation (2) were obtained in [20] from a fit to a set of six TDCSs with $E_1 = 5$ eV ($R = 7$) measured previously by the same group [14]. These values are compared with the ones obtained from the fitting of the present TDCS for $R = 7$ and $1/7$ in table 1.

The present values reported in table 1 are obtained as a weighted average among the values produced by fitting the experimental TDCS with equations (1) and (2). Among all the sets of parameters obtained by the fit we found a noticeable deviation from the average value in the case of the correlation width of the gerade amplitude for $E_1 = 5$ eV, $E_2 = 35$ eV and $\vartheta_1 = 30^\circ$ where both the three- or four-parameter best fits gave $\vartheta_{1/2} = 93 \pm 3$ and for $E_1 = 35$ eV, $E_2 = 5$ eV and $\vartheta_1 = 0^\circ$ where the three-parameter best fit gave $\delta = \pm 258 \pm 5^\circ$. For the sake of clarity only the TDCS obtained from the *practical parametrization* with four parameters are represented in figures 1(*a*) and (*b*) (full curves) and in the polar plots inserted in the top-left corner of the same figures. Only for the case $E_1 = 5$ eV, $E_2 = 35$ eV and $\vartheta_1 = 30^\circ$ was a rescaling factor of 0.88 applied to the curve calculated with the average values of the parameters. The results obtained with the three-parameter fit are comparable, but for the $E_1 = 35$ eV, $E_2 = 5$ eV and $\vartheta_1 = 0^\circ$ where the average value of δ produces a shape different to that produced experimentally. The ambiguity in the sign of δ can be resolved only via the measurement of the complementary TDCS with circularly polarized radiation [7]. As far as comparison with the data of [19] is concerned, an excellent agreement is found for the width of the correlation function and the ratio η, but the δ value differs by about 15°.

The experiments were compared with the theoretical predictions of the convergent close coupling (CCC) [21, 22] and 3C [23, 24] methods.

The CCC method is a fully numerical approach and relies on intensive computation. For the final state it solves the Schrödinger equation for a photoelectron-scattering system on the He^+ ion by employing the close-coupling expansion of the total wavefunction. The PDI results

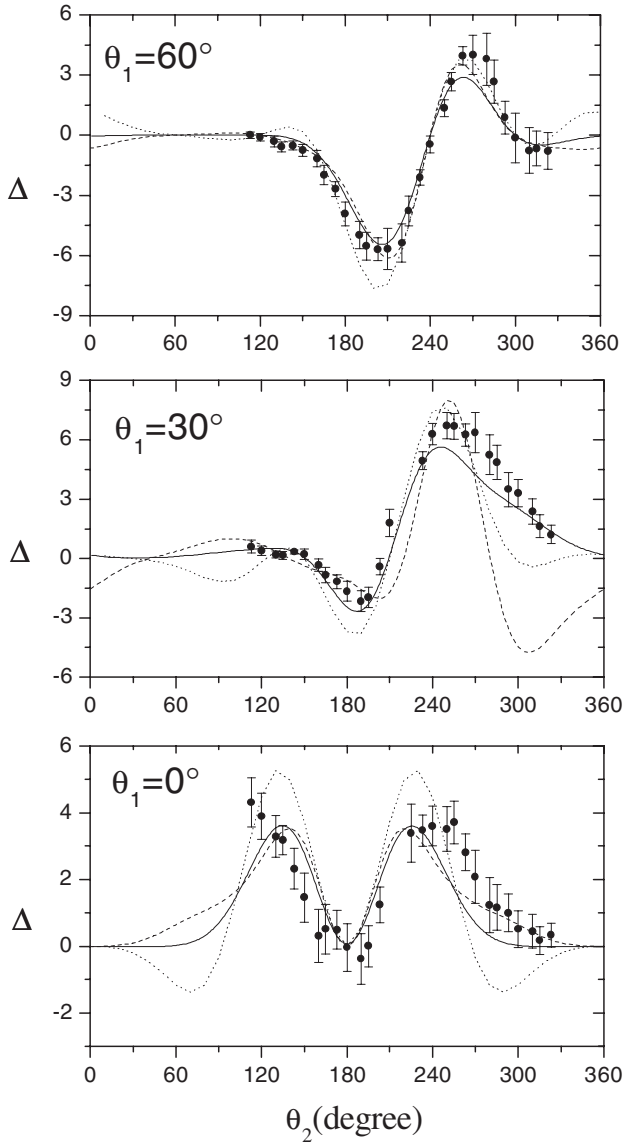

Figure 2. The difference, Δ, between the complementary TDCS (see equation (2)) compared with the theoretical data (dashed curve, CCC length form; dotted curve, 3C velocity form) and the values obtained from the TDCS representation according to the *practical parametrization* of [20] with four parameters (full curve).

from the electron impact ionization of the He^+ ion. The initial state is represented by a highly correlated Hylleraas-type wavefunction. The CCC integrated PDI cross sections agree with the experiment over a broad energy range [22]. Moreover the calculations in the three gauges differ by less than 5% and thus only the velocity-gauge calculation is shown in figures 1(*a*) and (*b*).

For the sake of comparison the amplitudes a_g and a_u derived from the CCC calculation were fitted with the Gaussian ansatz (2). The fitting parameters are presented in table 1 along with

the values used in the *practical parametrization*. Two substantially different width parameters are needed to fit the a_g and a_u amplitudes. Both values are consistent with those used in the *practical parametrization*. The other two parameters η and δ are also close to those obtained from the experiments. Moreover there is no ambiguity in the sign of δ in the CCC calculation.

In the 3C methods an analytical wavefunction where all the interactions in the final state are treated on an equal footing is used [23]. For the initial state a correlated wavefunction that fulfils the cusp condition was adopted. The present calculations were performed in the velocity gauge. In addition to these calculations we also employed the method proposed in [25], which accounted for the two-particle off-shell effects (on the total energy shell). Since these effects do not change either the shape of the TDCS or their relative intensity with respect to those obtained within the 3C model we did not include these additional results here.

The experiments have been normalized to the CCC calculation at $E_1 = 5$ eV, $\vartheta_1 = 60^\circ$ and $\vartheta_2 = 300^\circ$. The 3C calculation have been scaled by a factor 0.515 to the CCC one at the same angle. The experimental angular patterns of the TDCS are well reproduced by the two theories. However, in the case of $E_1 = 5$ eV the theories tend to overestimate the magnitude of the TDCS at $\vartheta_1 = 30^\circ$ and 0°. The disagreement of the presently measured TDCS with the CCC model can be completely removed by scaling the calculation down by a factor of 0.62. We note that a similar factor of 0.88 had to be applied to the practical parametrization to bring it towards the experiment at $\vartheta_1 = 30^\circ$.

Some discrepancies between the measured TDCS with the 3C calculation are observed. This calculation predicts the positions of the lobe shifted by a few degrees with respect to the experiment at $\vartheta_1 = 60^\circ$ and 30°, and intense side lobes at $\vartheta_1 = 0^\circ$. Looking at the *practical parametrization* it appears that the size of the side lobes at $\vartheta_1 = 0^\circ$ are determined by the a_g amplitude. Thus this term seems to be overestimated in the 3C calculation.

In the complementary case a reasonable agreement in the shape of the angular pattern as well as in the relative intensity is observed at $\vartheta_1 = 60^\circ$ and 30°. On the other hand, at $\vartheta_1 = 0^\circ$ different shapes are predicted by the two theories, neither of which agrees with the experimental observation. In this case *practical parametrization* gives an acceptable representation of the data, but a change in the relative phase shift δ is needed when only three parameters are used. The angular pattern predicted by the CCC model is reminiscent of the angular distribution with three lobes of the complementary case, while the one predicted by the 3C model has only one lobe. This latter pattern is expected when single-electron behaviour governs the PDI process. The experiment displays an angular pattern which is better represented by a three-lobe structure, although the central feature is not as pronounced as in the CCC calculations. Thus it appears that at $E = 40$ eV the PDI process is not yet dominated by one-electron behaviour. This conclusion is in agreement with a recent analysis by Kheifets [26] who showed that correlations become insignificant at excess energies exceeding 100 eV. On the other hand, if one would make a judgement based solely on the shape of the predicted [13] and measured [27] energy distribution of the photoelectrons, uncorrelated behaviour could be assumed at this low excess energy of 40 eV. This shows that measurement of the TDCS is a better tool for disentangling the details of the PDI process than measurement of the integral or less differential cross sections.

Discrepancies in the measured and calculated shapes of the TDCS for the complementary kinematics at $\vartheta_1 = 0^\circ$ has already been reported in the literature at lower excess energies. Bräuning *et al* [12] noted that the CCC theory predicts the shape of the TDCS which is slightly different from the experiment at $E_1 = 17$ eV, $E_2 = 3$ eV and $\vartheta_1 = 0^\circ$. In all other cases studied the CCC theory was consistent with the experimental data. On the other hand, the 3C theory was in good agreement with the experiment at the complementary kinematics at $\vartheta_1 = 0^\circ$ but disagreement was found at $E_1 = E_2$ and $E_1 = 3$ eV, $E_2 = 17$ eV. Very recently a new calculation by Malegat *et al* [28] predicted the TDCS for complementary kinematics at

$\vartheta_1 = 0^\circ$ consistent with the CCC results, thus the matter remains controversial.

Comparison of the experimental and theoretical Δ values in figure 2 confirms the previous observations. The general shape of this difference is well reproduced by the theories at all angles. However, at $\vartheta_1 = 30^\circ$ the CCC model predicts a narrower feature at about $\vartheta_2 = 250^\circ$ than that observed experimentally, while at $\vartheta_1 = 0^\circ$ the differences between the 3C calculations and the experimental data, already discussed in the description of figures 1(*a*) and (*b*), result in higher maxima and deeper minima in figure 2.

In summary, the TDCS of He at 40 eV excess energy were measured at unequal energy sharing for the complementary cases of $R = 7$ and $1/7$ and three different ϑ_1 values. Comparisons were made with the *practical parametrization* suggested by Cvejanovic and Reddish [20], and the two *ab initio* theories of CCC and 3C. *Practical parametrization* with four parameters gives an adequate description of the experiment. The only exception is the kinematics $E_1 = 5$ eV, $E_2 = 35$ eV and $\vartheta_1 = 30^\circ$ where the correlation factor of the gerade amplitude had to be modified and the full curve rescaled by a factor of 0.88. Comparison with CCC theory is also satisfactory if rescaling is made to different sets of the experimental TDCS. The exception is the complementary kinematics at $\vartheta_1 = 0^\circ$ where the CCC theory predicts a much more pronounced maximum in the TDCS at $\vartheta_2 = 180^\circ$. The 3C theory qualitatively describes the main features of the experiment but sometimes disagrees over the finer details. Our general conclusion is that complementary kinematics at a fixed-emission direction parallel to the electric light vector are the most challenging experimental conditions for theoretical PDI models at the present time.

In addition, our TDCS measurements show that at the excess energy of 40 eV the motion of the two photoelectrons is more correlated than expected solely on the basis of the measurements and calculations of the less-differential cross sections. This also shows that the transition from the highly correlated motion, typical of the threshold region, to a completely uncorrelated one is a gradual process which likely ends asymptotically [19, 24].

Acknowledgments

This work was partially supported by the 'INFM-Progetto Luce di Sincrotrone' (Application GAPH002S01). LA gratefully acknowledges stimulating discussions with S Cvejanovic (who also provided the original data of [14]). The authors thank A Martin and F Suran for their help in setting up the the power-supply system of the multicoincidence spectrometers, and M Mastropietro for contributing to the development of the counting electronics.

References

[1] Kossmann H, Schmidt V and Andersen T 1988 *Phys. Rev. Lett.* **58** 1620
[2] Ullrich J, Moshammer R, Dörner R, Jagutzki O, Mergel V, Schmidt-Böcking H and Spielberg L 1997 *J. Phys. B: At. Mol. Opt. Phys.* **30** 2917
[3] Schwarzkopft O, Krässig B, Elminger J and Schmidt V 1993 *Phys. Rev. Lett.* **70** 3008
[4] Huetz A and Mazeau J 2000 *Phys. Rev. Lett.* **85** 530
[5] Gulley N 1997 *PhD Thesis* University of Manchester
[6] Avaldi L, Battera G, Camilloni R, Coreno M, DeSimone M, Prince K C, Turri G, Zitnik M and Stefani G 1999 *21st Int. Conf. Proc. on Electronic and Atomic Collisions (Tokyo, 1999) Book of Abstracts* eds Y Itikawa, K Okuno, H Tanaka, A Yagashita and M Matsuzawa p 23
[7] Briggs J S and Schmidt V 2000 *J. Phys. B: At. Mol. Opt. Phys.* **33** R1
[8] King G C and Avaldi L 2000 *J. Phys. B: At. Mol. Opt. Phys.* **33** R215
[9] Huetz A, Selles P, Waymel D and Mazeau J 1991 *J. Phys. B: At. Mol. Opt. Phys.* **24** 1917
[10] Dawber G, Avaldi L, McConkey A G, Rojas H, MacDonald M A and King G C 1995 *J. Phys. B: At. Mol. Opt. Phys.* **28** L271

[11] Lablanquie P, Mazeau J, Andric L, Selles P and Huetz A 1995 *Phys. Rev. Lett.* **74** 2192
[12] Bräuning H *et al* 1998 *J. Phys. B: At. Mol. Opt. Phys.* **31** 5149
[13] Proulx D and Shakeshaft R 1993 *Phys. Rev.* A **48** R875
[14] Cvejanovic S, Wightman J P, Reddish T J, Maulbetsch F, MacDonald M A, Kheifets A S and Bray I 2000 *J. Phys. B: At. Mol. Opt. Phys.* **33** 265
[15] Melpignano P, Di Fonzo S, Bianco A and Jark W 1995 *Rev. Sci. Instrum.* **66** 2125
[16] Blyth R R *et al* 1999 *J. Electron Spectrosc. Relat. Phenom.* **101–103** 959
[17] Wehlitz R, Langer B, Berrah N, Whitfield S B, Viefhaus J and Becker U 1993 *J. Phys. B: At. Mol. Opt. Phys.* **26** L783
[18] Lindle D W, Heiman P A, Ferret T A, Kobrin P H, Truesdale C M, Becker U, Kerkhoff H G and Shirley D A 1986 *Phys. Rev.* A **33** 319
[19] Cvejanovic 2001 Private communication
[20] Cvejanovic S and Reddish T J 2000 *J. Phys. B: At. Mol. Opt. Phys.* **33** 4691
[21] Kheifets A S and Bray I 1998 *J. Phys. B: At. Mol. Opt. Phys.* **31** L447
Kheifets A S and Bray I 1998 *Phys. Rev. Lett.* **81** 4588
[22] Kheifets A S and Bray I 1998 *Phys. Rev.* A **58** 4501
[23] Bräuner M, Briggs J S and Klar H 1989 *J. Phys. B: At. Mol. Opt. Phys.* **22** 2265
[24] Maulbetsch F and Briggs J S 1994 *J. Phys. B: At. Mol. Opt. Phys.* **27** 4095
[25] Berakdar J 1997 *Phys. Rev. Lett.* **78** 2712
[26] Kheifets A S 2001 *J. Phys. B: At. Mol. Opt. Phys.* **34** L247
[27] Wehlitz R, Heiser F, Hemmers O, Langer B, Menzel A and Becker U 1991 *Phys. Rev. Lett.* **67** 3764
[28] Malegat L, Selles P and Kazansky A K 2000 *Phys. Rev. Lett.* **85** 4450